JACS
JOURNAL OF THE AMERICAN CHEMICAL SOCIETY

Subscriber access provided by UNIV OF ESSEX

Article

Hetero Cu(III)-Pd(II) Complex of a Dibenzo[g,p]chrysene Fused Bis-dicarbacorrole with Stable Organic Radical Character

Xian-Sheng Ke, Yongseok Hong, Peiyu Tu, Qing He, Vincent M. Lynch, Dongho Kim, and Jonathan L. Sessler

J. Am. Chem. Soc., **Just Accepted Manuscript** • DOI: 10.1021/jacs.7b09167 • Publication Date (Web): 30 Sep 2017

Downloaded from http://pubs.acs.org on September 30, 2017

Just Accepted

“Just Accepted” manuscripts have been peer-reviewed and accepted for publication. They are posted online prior to technical editing, formatting for publication and author proofing. The American Chemical Society provides “Just Accepted” as a free service to the research community to expedite the dissemination of scientific material as soon as possible after acceptance. “Just Accepted” manuscripts appear in full in PDF format accompanied by an HTML abstract. “Just Accepted” manuscripts have been fully peer reviewed, but should not be considered the official version of record. They are accessible to all readers and citable by the Digital Object Identifier (DOI®). “Just Accepted” is an optional service offered to authors. Therefore, the “Just Accepted” Web site may not include all articles that will be published in the journal. After a manuscript is technically edited and formatted, it will be removed from the “Just Accepted” Web site and published as an ASAP article. Note that technical editing may introduce minor changes to the manuscript text and/or graphics which could affect content, and all legal disclaimers and ethical guidelines that apply to the journal pertain. ACS cannot be held responsible for errors or consequences arising from the use of information contained in these “Just Accepted” manuscripts.

ACS Publications

Journal of the American Chemical Society is published by the American Chemical Society. 1155 Sixteenth Street N.W., Washington, DC 20036

Published by American Chemical Society. Copyright © American Chemical Society. However, no copyright claim is made to original U.S. Government works, or works produced by employees of any Commonwealth realm Crown government in the course of their duties.

Hetero Cu(III)-Pd(II) Complex of a Dibenzo[*g,p*]chrysene Fused Bis-dicarbacorrole with Stable Organic Radical Character

Xian-Sheng Ke[†], Yongseok Hong[‡], Peiyu Tu[†], Qing He[†], Vincent M. Lynch[†], Dongho Kim[*‡], and Jonathan L. Sessler[*†]

[†] Department of Chemistry, The University of Texas at Austin, Austin, Texas 78712-1224, United States.

[‡] Department of Chemistry, Yonsei University, Seoul 03722, Korea

KEYWORDS. Radical, carbaporphyrins, corroles, hetero multi-nuclear complexes, antiaromaticity.

ABSTRACT: Bis-dicarbacorrole (**bis-H_3**) with two adj-CCNN subunits was synthesized by incorporating a dibenzo[*g,p*]chrysene moiety into the macrocyclic structure. The two trianionic cores in **bis-H_3** can stabilize two Cu(III) ions (**bis-Cu**) or concurrently a Cu(III) cation and a Pd(II) ion in the form of a hetero bis-metal complex (**mix-Cu/Pd**). As prepared, **mix-Cu/Pd** displays organic π radical character, as confirmed by various techniques, including electron paramagnetic resonance (EPR) spectroscopy, cyclic voltammetry (CV), femtosecond transient absorption (fs-TA) measurements and DFT calculations. Radical formation is ascribed to one-electron transfer from the dicarbacorrole backbone to the Pd center allowing the d^8 Pd(II) center to be accommodated in a square planner coordination geometry. Nucleus-independent chemical shift (NICS) and anisotropy of the induced current density (AICD) calculations provide support for the conclusion that **bis-H_3** and **bis-Cu** both display antiaromatic character and contain two formally 16 π-electron dicarbacorrole subunits. On this basis, we suggest that **mix-Cu/Pd** is best considered as containing a fused 15 π-electron nonaromatic radical subunit and a 16 π-electron antiaromatic subunit. The spectroscopic observations are consistent with these assignments.

Introduction

Stable organic radicals with open-shell character show unique electronic properties[1] that are very different from traditional closed-shell π-conjugated systems. Such radical systems have many potential applications in organic electronics,[2] molecular spintronics,[3] non-linear optical materials,[4] and energy storage.[5] The inherent complexity of open-shell radical systems and their potential utility across a number of application areas provide an incentive to make and study novel molecular systems with radical properties. However, the design and synthesis of stable organic radicals is challenging. In general open shell systems are characterized by thermodynamic instability and high kinetic reactivity. This makes such systems very difficult to make and manipulate. Oligopyrrolic macrocycles, such as porphyrins, metalloporphyrins, and expanded porphyrins, are known to stabilize radicals as the result of their π-electron delocalized structures.[6] Although of potential interest in terms of both basic chemistry and for the development of magnetic materials,[7] stable organic radicals based on multimetallic porphyrins are still rare. To date, homo bis-metallic complexes, including the bis-Pd complexes of a [28]hexaphyrin[8] and a contracted doubly N-confused dioxohexaphyrin,[9] a bis-Cu complex of a siamese-twin porphyrin,[10] and a bis-Zn complex of a doubly-linked corrole dimer,[11] have been reported that display ligand-centered (i.e., primarily organic) radical character. Here, we report what to our knowledge is the first example of a hetero bis-metallic porphyrinoid system showing stable organic radical character. We also show that depending on the coordination chemistry, it is possible to obtain a hetero bis-metallic complex that is formally antiaromatic and lacking radical character. This ability to stabilize different metalated and electronic forms is made possible by use of a new fused dicarbacorrole.

Carbaporphyrins are porphyrin analogues in which one or more nitrogen atoms within the macrocyclic cavity is replaced by a carbon atom.[12] Examples of such systems include the benziporphyrins[13], oxybenziporphyrins,[14] tropiporphyrins,[15] azuliporphyrins,[16] napthiporphyrins,[17] N-confused porphyrins,[18] neo-confused porphyrins,[19] and pyreniporphyrin.[20] Depending on the specific structure in question, carbaporphyrins can display π-conjugation pathways that differ from the traditional 18 π-electrons circuits typically found in all-pyrrolic porphyrins. The presence of inward pointing C-H moieties can also permit formation of novel metal complexes.[12] Although mono-metal complexes of carbaporphyriniods with one or more C donors have been extensively explored,[12] complexes containing more than one coordinated cation have been less well studied. Osuka, Furuta, Kim and coworkers have reported the use of expanded porphyrins,[21] such as hexaphyrin/N-confused hexaphyrin, octaporphyrin and nonaphyrin, as ligands to stabilize bis- and tri-metal complexes with group 10 and 11 metals.[22] Lash and coworkers reported an unusual tris-palladium sandwich complex obtained from a simple dicarbaporphyrin ligand.[23] However, to the best of our knowledge, none of these reported systems has displayed organic radical character. The goal of the present study, therefore, was to create a new carboporphyrin analogue that could be used to stabilize a hetero bis-metallic complex with organic radical character. As detailed below, the use of a new carbaporphyrinoid that contains two adjoining CCNN coordination environments has allowed this goal to be accomplished.

The present system differs from previous reported 1,4-phenylene-bridged expanded porphyrins[24] in that it contains a large dibenzo[*g*,*p*]chrysene moiety within its core structure. This creates two trianionic cavities, which are similar to those in corrole,[25] a contracted porphyrin known to stabilize higher oxidation states of metal ions.[26] The present bis-dicarbacorrole (**bis-H$_3$**) acts as a ligand that can stabilize complexes containing one or two Cu(III) ions (**mono-Cu** and **bis-Cu**). It can also stabilize a mixed Pd(II)-Cu(III) complex, **mix-Cu/Pd**. On the basis of its near-silent ^{1}H and ^{19}FNMR signals, an observed EPR signal at *g* = 2.00, and NICS and ACID calculations **mix-Cu/Pd** is considered to contain both 15 π-electron nonaromatic neutral radical and a 16 π-electron antiaromatic dicarbacorrole-like subunits.

Scheme 1 Synthesis of bis-H$_3$ and its metal complexes.^{a,b}

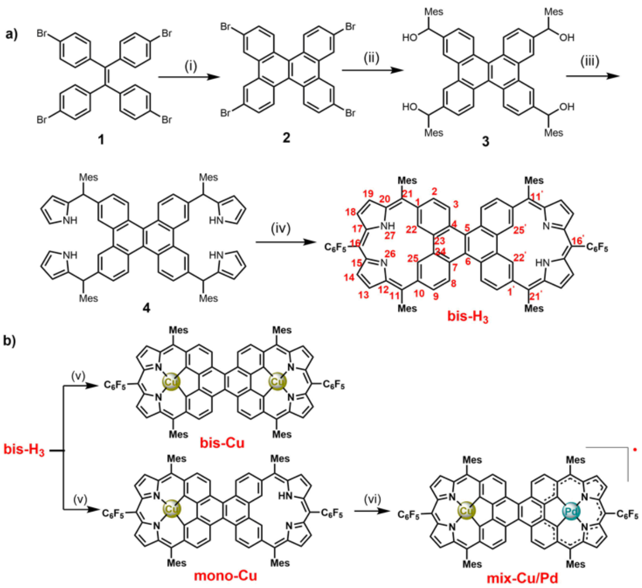

^{a}Conditions for the synthesis of **bis-H$_3$**: (i) DDQ and trifluoromethanesulfonic acid in dichloromethane (DCM) with stirring at 0 °C for 1 h, then room temperature for 4 h, 30%, (ii) *n*-BuLi in THF, -78 °C, 1 h, then mesitaldehyde, -78 °C, 1 h, 55%; (iii) pyrrole and BF$_3$•OEt$_2$, reflux, 20 h, 60%; (iv) pentafluorobenzaldehyde and BF$_3$•OEt$_2$ in dry DCM, room temperature, 2.5 h, then DDQ, room temperature, 0.5 h, 8%. ^{b}Conditions for the synthesis of metal complexes: (v), Cu(OAc)$_2$•H$_2$O in CHCl$_3$, reflux, 48 h. The isolated yields for **mono-Cu** and **bis-Cu** are 46% and 33%, respectively, (vi) Pd(PhCN)$_2$Cl$_2$ in PhCN, 180 °C, 2h, 89%. Mes and C$_6$F$_5$ denote mesityl and pentafluorophenyl groups, respectively.

Results and Discussion

The synthesis of **bis-H$_3$** is summarized in **Scheme 1a**. Firstly, a trifluoromethanesulfonic acid-promoted oxidative fusion of tetra(*p*-bromophenyl)ethene[27] **1** was carried out using 2,3-dichloro-5,6-dicyano-p-benzoquinone (DDQ) to form the tetrabrominated dibenzo[*g*,*p*]chrysene **2**. The tetracarbinol **3** was then synthesized from **2** by reaction with mesitaldehyde in the presence of *n*-butyllithium. Heating **3** in pyrrole at reflux provided the tetrapyrrole intermediate **4**. Finally, a boron trifluoride etherate-catalyzed condensation reaction between **4** and pentafluorobenzaldehyde, followed by oxidation with DDQ, produced the target **bis-H$_3$** in 8% yield. **Bis-H$_3$** was characterized by ^{1}H, ^{19}F, 2D-correlation spectroscopy (COSY) NMR spectroscopies, UV-vis absorption spectroscopy, high-resolution ESI mass spectrometry and single crystal X-ray diffraction analysis (Figures S26-S29 and S40).

Suitable single-crystals of **bis-H$_3$** were grown in CH$_2$Cl$_2$/n-hexane and the resulting X-ray structure unambiguously confirmed the formation of **bis-H$_3$**. As shown in Figure 1, the central dibenzochrysene is distorted from the plane defined by the flanking dipyrromethene subunits. The dihedral angles between two inner benzenes and the dipyrromethene plane are 23.0° (Figure 1b), which is bigger than that in reported in a different dicarbaporphyrinoid.[28] The C(10)-C(11) and C(1)-C(21) bond lengths were 1.473 and 1.472 Å (Figure 1a), respectively, indicating that the dibenzochrysene moiety is bound to both dipyrromethene units through what are predominantly single bonds. However, all non-hydrogen atoms in the core appear to be sp^2 hybridized.

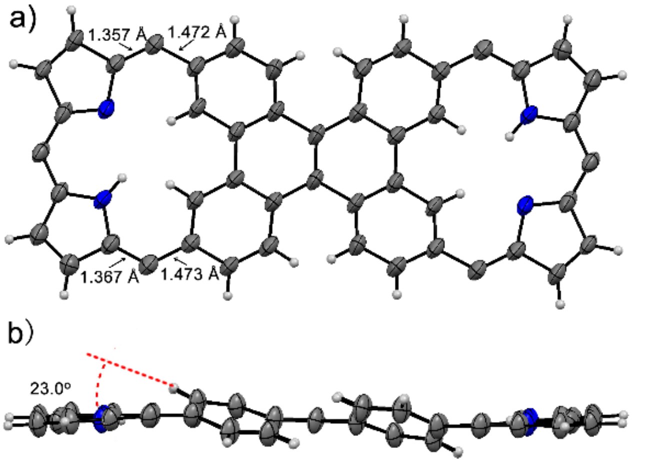

Figure 1. Single crystal X-ray diffraction structure of **bis-H$_3$**; (a) top and (b) side views. Thermal ellipsoids are scaled to the 50% probability level. *meso*-Aryl substituents are omitted for clarity.

The ^{1}H NMR spectrum of **bis-H$_3$** was recorded in CD$_2$Cl$_2$. (Figure 2) There are two doublets located at 5.48 and 5.79 ppm, which are assigned to the pyrrolic β-Hs. Signals at 6.02 and 7.42 ppm are also seen that assigned to the outer CHs in the dibenzo[*g*,*p*]chrysene moiety. A combination of D$_2$O exchange (Figure S28) and H-H COSY experiments (Figure S29) revealed broad resonances at 14.49 and 15.97 ppm that were assigned to the inner CH and NH groups, respectively (Figure 2). The average chemical shift differences between the pyrrolic NH and β-H protons (Δδ) and the dibenzo[*g*,*p*]chrysene inner CH and outer CH (Δδ') were found to be 10.3 and 7.8 ppm, respectively. These distinct differences between the chemical shifts were taken as initial evidence that **bis-H$_3$** possesses antiaromatic character.

The UV–Vis-NIR absorption spectrum of **bis-H$_3$** in toluene is consistent with this assignment. An intense absorption feature at 425 nm with two shoulders located at 379 and 502 nm, along with a weak, broad absorption band centered at ca. 780 nm, are seen (Figure 3). The absorption spectrum is quite similar but slightly red-shifted to that of phenanthriporphyrin,[29] a previously characterized antiaromatic system.

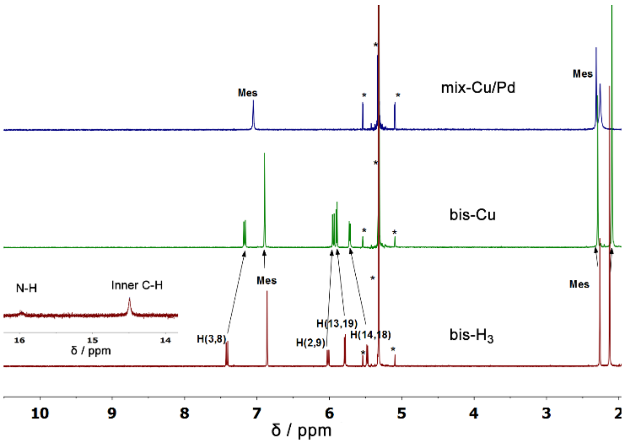

Figure 2. ^{1}HNMR spectra of **bis-H$_3$**, **bis-Cu** and **mix-Cu/Pd** recorded in CD_2Cl_2 at room temperature. In the symmetric systems, the labeling refers to the features for a single corrole-like subunit. Asterisks indicate peaks arising from the solvent.

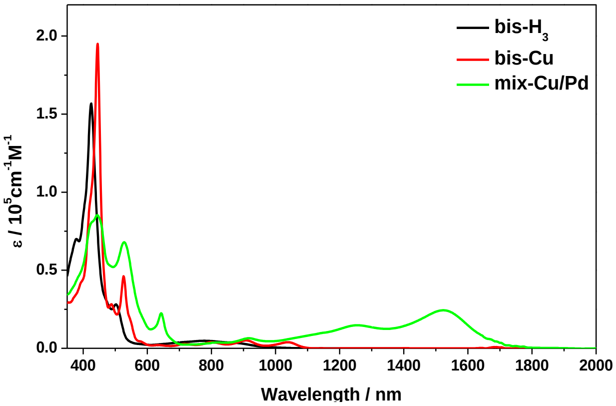

Figure 3. UV–vis-NIR absorption spectra of **bis-H$_3$**, **bis-Cu** and **mix-Cu/Pd** recorded in toluene.

Further support for the proposed antiaromaticity of **bis-H$_3$**, came from nucleus-independent chemical shift (NICS) and anisotropy of the induced current density (ACID) calculations. (Figures S9-S11). The DFT optimized structure used for these calculations proved in good agreement with the crystal structure. (Figure S6) The $NICS_{ZZ}$ values were visualized using the program Multiwfn_2.9.9[30] to produce an isochemical shielding surface (ICSS) (Figure 5a and S10). Using this visualization approach, positive and negative NICS values are shown in blue and red, respectively. **Bis-H$_3$** shows positive $NICS_{zz}$ values (red) within the inner circuit along the XY plane ($NICS_{zz}$ (Z = 0)). To avoid σ-bond interactions with atoms, plots were also constructed in the XZ plane ($ICSS_{zz}$ (Y = 0)). Now the inside is characterized by negative values, while positive values are seen for the outside. Such findings are consistent with the assignment of **bis-H$_3$** as antiaromatic. In the $ICSS_{zz}$ (Y = 0) plot, a node is seen at the center of the two subunits, leading us to propose that there are two individual π-conjugation pathways within **bis-H$_3$**. Various NICS(0) values within **bis-H$_3$** were also calculated (Figure S9). All of the NICS(0) values within the inner circuits were positive, as expected for an antiaromatic system. ACID plots of **bis-H$_3$** revealed paratropic antiaromatic current flow within the independent circuits of the two subunits, with the independence resulting in part from the tilted nature of dibenzochrysene bridging element (Figure S11).

To rationalize the π-conjugation pathway along the individual circuits, harmonic oscillator model of aromaticity (HOMA) calculations were carried out for the possible pathways using the optimized structure.[31] HOMA values are defined in terms of the normalized sum of the squared deviations of bond lengths from the optimal values along a given π-conjugation pathway.[32] The cannical aromatic system, benzene, has a HOMA value = 1, while the HOMA value = 0 is for a nonaromatic compound. In the case of **bis-H$_3$**, the HOMA values of 0.503 and 0.510 for the antiaromatic 16 and 20 π-electron conjugation pathways, respectively, are similar to that (0.549) calculated for a what might be expected to be a competing 38 π-electron aromatic pathway. On this basis, we suggest that the putative global conjugation is broken due to the presence of central dibenzochrysene (Figure S17) and that **bis-H$_3$** has antiaromatic character (16 π + 16 π = 32 π-electrons) and can be viewed as being a kind of fused corrole dimer.[33]

Carbaporphyrinoids with adj-CCNN cores are known to stabilize higher oxidation state of metal ions or main group elements, such as Cu(III),[28,34] Ag(III),[34a] and P(V).[29] Pd complexes of carbaporphyrinoids have also been extensively explored.[23,35] Metalation of **bis-H$_3$** with excess $Cu(OAc)_2$•H_2O in $CHCl_3$ at reflux give **bis-Cu** and **mono-Cu** in 33% and 46% yield, respectively (**Scheme 1b**). Reaction of **mono-Cu** with bis(benzonitrile)palladium chloride ($Pd(PhCN)_2Cl_2$) in PhCN at 180 °C (**Scheme 1b**) produced a red-brown fraction that could be isolated via normal silica chromatographic purification. A high-resolution ESI mass spectrometric analysis of the product revealed a parent ion peak at *m/z* 1627.3025 (calcd for $C_{96}H_{60}CuF_{10}N_4Pd$ $[M]^+$: 1627.3009, Figure S40), as would be the formation of a hetero metal complex containing both Cu and Pd centers. The **bis-Cu** and **mix-Cu/Pd** complexes were further characterized by UV-vis-NIR absorption spectroscopy, ^{1}H and ^{19}F NMR or EPR spectroscopies, and single crystal X-ray diffraction analysis (Figures S4-S5, S33-S37 and S42-S43).

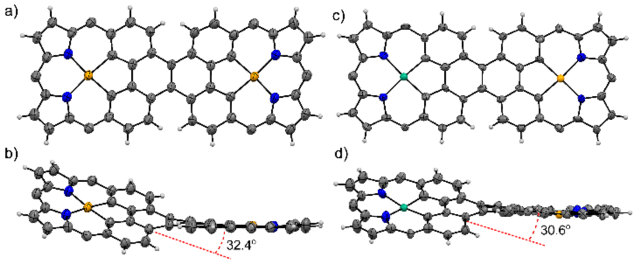

Figure 4. Single crystal X-ray diffraction structures of **bis-Cu** and **mix-Cu/Pd**. a) Top and b) side views of the **bis-Cu**, c) Top and d) side views of the **mix-Cu/Pd**. For **mix-Cu/Pd**, the Cu and Pd ions are disordered over the two possible locations in the macrocycle and only one population is shown. Thermal ellipsoids are scaled to the 50% probability level. *meso*-Aryl groups are omitted for clarity.

As can be seen from an inspection of Figure 4, both **bis-Cu** and **mix-Cu/Pd** are characterized by twisted conformations in solid state displaying a greater degree of distortion than seen in the starting free base ligand, **bis-H$_3$**. Dihedral angles of 32.4° and 30.6 °, respectively, are seen between the two corrole subunits (defined by the mean plane of the CCNN at-

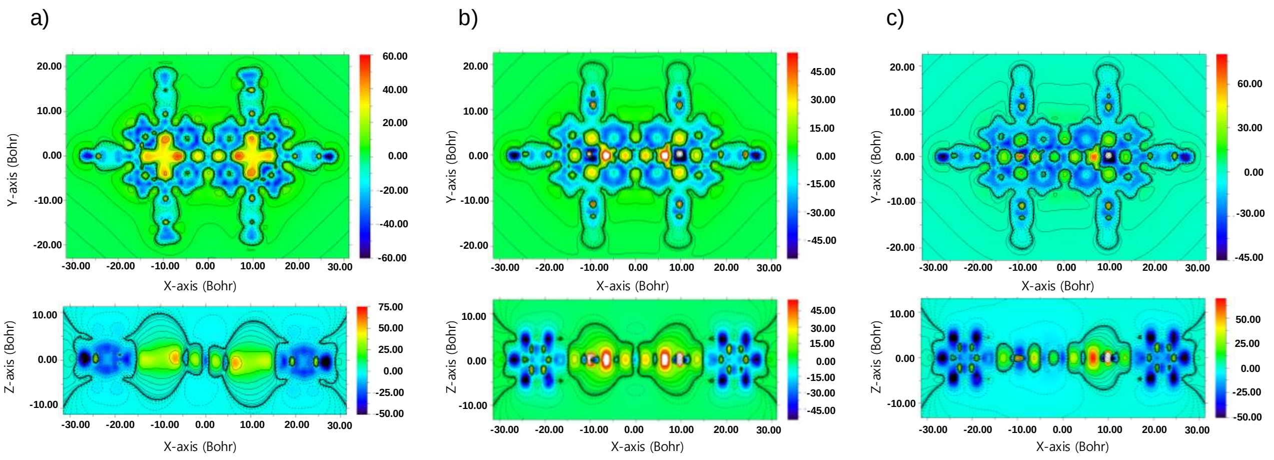

Figure 5. ICSS$_{zz}$ plots of a) **bis-H$_3$**, b) **bis-Cu**, and c) **mix-Cu/Pd**. Blue and red contour colors denote negative and positive NICS$_{zz}$ values, respectively. The upper and lower panels represent ICSS$_{zz}$ (Z = 0) and ICSS$_{zz}$ (Y = 0), respectively

oms). In these metal complexes, the Pd and Cu ions are located within the corresponding adj-CCNN cores with square-planar coordination geometries and no axial ligands being seen in the crystal structure. The absence of axial ligands, the presence of what are square-planar coordination geometries about the metal centers, and metal-C and metal-N bond lengths (Figure S21) that are in good agreement with those reported for Cu(III) dicarbaporphyrinoid complexes with adj-CCNN cores[28] leads us to assign the oxidations of the copper ions in both **bis-Cu** and **mix-Cu/Pd** as +3 (d^8). On the other hand, the high reactivity and propensity for Jahn-Teller distortion away from pure octahedral geometries seen in the case of d^7 Pd(III) complexes,[36] leads us to suggest that the oxidation state of the Pd ion in **mix-Cu/Pd** is +2 (d^8). Further analyses were then carried out to confirm or refute this preliminary assignment as discussed below.

The ^{1}HNMR spectra of both **bis-Cu** and **mix-Cu/Pd** were recorded in CD$_2$Cl$_2$ (cf. Figure 2). The ^{1}HNMR spectrum of **bis-Cu** bears resemblance to that of **bis-H$_3$**. However, many of the signals are slightly upfield shifted. The same proved true in the case of **mono-Cu** (Figure S30). These findings are consistent with both copper-only complexes being diamagnetic and the ligand possessing antiaromatic character analogous to that seen in the original doubly trianionic ligand, **bis-H$_3$**. In contrast to the sharp signals seen for **bis-Cu** and **mono-Cu**, only the *meso*-mesityl proton signals are readily observable in the spectrum of **mix-Cu/Pd** either at room temperature (Figure 2) or -80 °C (Figure S36). These findings were mirrored in the case of the ^{19}F NMR spectra, where only a weak signal for the o-F of the *meso*-pentafluorophenyl groups could be observed both at room temperature and -80 °C (Figure S37). These findings are consistent with the Pd center being in the +2 oxidation state and the ligand as a whole having radical character to provide for the necessary charge balance.

The EPR spectrum of **mix-Cu/Pd** in toluene solution was then measured at 290 K (Figure 6a). A single peak was observed at *g* = 2.00. This is as would be expected for a typical organic monoradical (S =1/2). No discernible signals corresponding to $\Delta m_S = \pm 2$ are seen in the half-field region (Figure S4). Both **bis-Cu** and **mono-Cu** are EPR silent over the 90-360 K temperature range (Figure S5). This is consistent with their proposed diamagnetic nature and the +3 oxidation state assigned to the Cu ions and is in accord with previous reports of Cu(III) dicarbacorrole complexes characterized by an adj-CCNN coordination environment.[28] In preliminary work, the mixed free-base mono-palladium complex of **bis-H$_3$** was prepared; it also gave rise to an EPR spectrum consistent with radical character (cf. Figure S4).

The absorption spectrum of **bis-Cu** recorded in toluene bears resemblance to that of **bis-H$_3$** but is characterized by a more intense band at ca. 445 nm and a new shoulder at ca. 526 nm (Figure 3). Discernible NIR bands, which could originate from slightly enhanced excitonic coupling between the two subunits, are also seen. In contrast to both **bis-Cu** and **mono-Cu** (Figure S1) the absorption spectrum of **mix-Cu/Pd** is characterized by broadened and red-shifted spectral features, as well as broad NIR bands centered at 1255 and 1524 nm. (Figure 3) The relatively strong NIR features are typical for radical species and reflect the small energy gap between the singly occupied molecular orbital (SOMO) and the singly unoccupied molecular orbital (SUMO). The change in the absorption spectrum of **mix-Cu/Pd** in toluene solution was monitored as a function of time under ambient conditions. Over a period of 120 h little discernible change as seen (Figure S2), leading us to suggest that the complex is stable on the laboratory time scale.

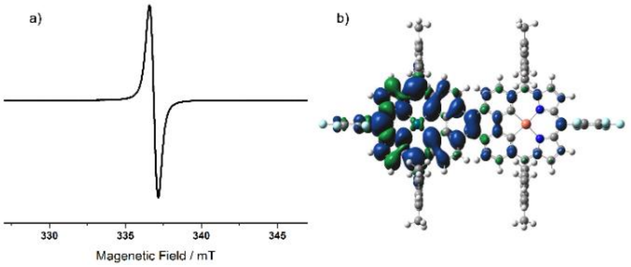

Figure 6. a) X-band EPR spectra of **mix-Cu/Pd** (1.0 mM in toluene) at 290 K. Instrument parameters: ν = 9.44 GHz, modulation frequency 100 kHz, modulation amplitude 2.0 G, microwave power 2.00 mW. b) Spin density map of **mix-Cu/Pd** calculated at the uM06/LANL2DZp level. Similar results were obtained when the calculation was carried out at the uB3LYP/IANI2DZp level (cf. Figure S20).

The redox properties of **bis-H$_3$**, **bis-Cu** and **mix-Cu/Pd** were studied by means of cyclic voltammetry (CV) carried out in CH$_2$Cl$_2$ containing 0.1 M NBu$_4$PF$_6$ as the electrolyte. The

CVs of both **bis-H$_3$** and **bis-Cu** are characterized by oxidation waves in the region of ca. +0.2 and +0.5 V vs Fc/Fc$^+$, as well as reduction waves around -1.31 to -1.39 V (Figure 7). Compared with **bis-H$_3$** and **bis-Cu**, the first oxidation wave of **mix-Cu/Pd** undergoes a modest cathodic shift (to + 0.14 V), while the first reduction wave undergoes a very substantial anodic shift and appears at -0.30 V. Thus, the gap between the first oxidation and reduction potentials ($\Delta E=E^{1}_{Ox}-E^{1}_{Red}$) based on the CV data decrease from ca. 1.63 and 1.51 V in the case **bis-H$_3$** and **bis-Cu** to 0.44 V in **mix-Cu/Pd**. Such an energetic reduction would account for the strongly red-shifted absorption features seen for **mix-Cu/Pd** (λ_{max} = 1524 nm, Figure 3). A small ΔE (0.44 V) is also a typical character for open shell organic radical species.[6k,9,11]

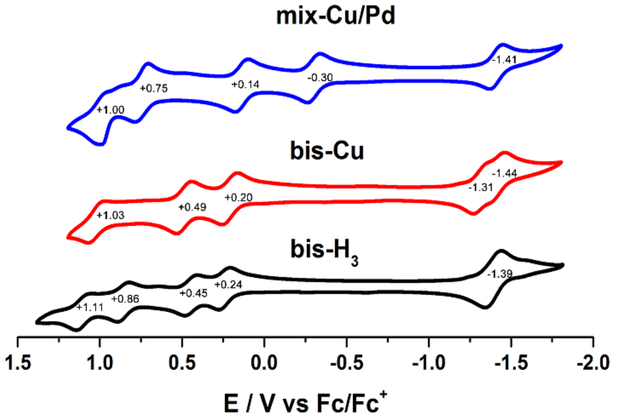

Figure 7. Cyclic voltammograms of **bis-H$_3$**, **bis-Cu**, and **mix-Cu/Pd** in CH_2Cl_2 containing 0.1 M NBu_4PF_6. The Fc/Fc$^+$ couple was used as an external reference and the scan rate is 50 mV/s.

To investigate the excited state dynamics of **bis-H$_3$**, **bis-Cu**, and **mix-Cu/Pd**, visible (VIS) femtosecond transient absorption (TA) studies were carried out in toluene (Figure S3). In the case of **bis-H$_3$**, the TA spectra decayed with two time components with half-lives of 0.3 and 8.6 ps, respectively (Figure S3). The TA spectra of **bis-Cu** was similar with the two decay components having half-lives of 1.2 and 8.9 ps, respectively (Figure S3). The two decay components seen in the case of both **bis-H$_3$** and **bis-Cu** are assigned to 1) internal conversion from the higher excited state to the lowest excited singlet state and 2) decay of the S_1 state, respectively, and are typical of what are seen for previous studies on porphyrin tapes or hybrid tapes.[37] The TA decay profile of **mix-Cu/Pd** could also be fit to a double exponential, yielding decay constants of 0.3 and 5.0 ps, respectively (Figure S3). The relatively short excited state lifetime is consistent with the radical nature of **mix-Cu/Pd**.[38]

NICS and ACID calculations were performed so as to obtain further insights into the (anti)aromaticity of the metal complexes (Figure 5, S9 and S12-16). ISCC$_{zz}$ (Z = 0) plots for **bis-Cu** shows positive values (red and yellow color) inside the central macrocyclic cavities, while ISCC$_{zz}$(Y= 0) plots also reveal positive features within the ring (Figure 5b). Similar features were seen for **bis-H$_3$** (Figure 5a). Furthermore, the NICS(0) values at the various positions are positive, supporting the antiaromaticity proposed for **bis-Cu** (Figure S9). ACID plots for **bis-Cu** exhibit paratropic antiaromatic current flows along the individual subunits (Figure S15), which is further consistent with the proposed antiaromaticity. The dominant π-conjugation pathway was inferred from various HOMA calculations (Figure S18). In analogy to what was found for **bis-H$_3$** (vide supra), the HOMA values for the 16 and 20 π-electron conjugation paths are almost the same as for a more global 38 π-electron conjugation pathway, which again is taken as an indication that antiaromatic (16 π + 16 π = 32 π-electron) peripheries dominate within individual subunits (Figure S18).

In contrast to what was seen for **bis-H$_3$** and **bis-Cu**, the ISCC$_{zz}$ (Y = 0) plot for **mix-Cu/Pd** indicates an asymmetric NICS$_{zz}$ distribution between the two subunits. In the NICS$_{zz}$ (Y = 0) plot, (Figure 5c) the Cu-bound side (right) resembles that of **bis-Cu**, while the Pd-containing side (left) shows significantly decreased positive values that reveal nonaromatic nature of Pd(II) side.[9] The NICS(0) values are consistent with the NICS$_{zz}$ plots (Figure S12). A detailed analysis of the HOMA values reveals that those for the Pd(II) portion are smaller than those for the Cu(III) side of the mixed metal complex. In addition, **mix-Cu/Pd** overall is characterized by a smaller HOMA value than either **bis-H$_3$** or **bis-Cu**, which is taken as an indication that the global π-conjugation pathway is less efficient. (Figure S19). The spin density of **mix-Cu/Pd**, obtained from calculations made for a doublet state (Figure 6b), provide support for the notion that the bulk of the spin density is localized on the Pd-containing portion of **mix-Cu/Pd**.

The above combination of experiment and calculations leads to the reasonable inference that most of the radical character is localized on this portion of the ligand and is predominantly organic in nature. The requisite ligand oxidation allows the palladium center to remain in the +2 oxidation state and adopt a d^8 square planar coordination geometry. Such a ligand centered oxidation is reasonable in light of the relatively low first oxidation potential of the free ligand (+ 0.24 V vs Fc/Fc$^+$, Figure 7) and similar findings made in the case of the bis-Pd complex of a doubly N-confused dioxohexaphyrin.[9] On this basis, we propose that **mix-Cu/Pd** is best considered as consisting of fused 15 π-electron nonaromatic and 16 π-electron antiaromatic subunits that involve the Pd(II) and Cu(III) complexed portions of the macrocycle, respectively.

Conclusion

In summary, we have synthesized and characterized the first bis-dicarbacorrole with two adj-CCNN cores. The bis-corrole ligand, containing a dibenzo[*g*,*p*]chrysene fusion element, can coordinate both Cu(III) and Pd(II) ions to form the first hetero bis-metal complex **mix-Cu/Pd** stabilized using a two-compartment porphyrin analogue. This complex displays stable organic radical character and supports the two metal centers in different oxidation states (+2 vs. +3). The present work thus underscores how ligand design may be used to create mixed metal complexes that allow both unusual metal- and ligand-centered oxidation states to be attained. The resulting systems are likely to further our understanding of the interplay between ligand electronics and metal coordination chemistry, as well as features that allow for the stabilization of formally antiaromic π-conjugation pathways.

ASSOCIATED CONTENT

Supporting Information

Synthesis and characterization details, NMR, supporting photophysical measurements, DFT calculation details, and X-ray experimental details. This material is available free of charge via the Internet at http://pubs.acs.org.

AUTHOR INFORMATION

Corresponding Author

sessler@cm.utexas.edu; dongho@yonsei.ac.kr

Notes
The authors declare no competing financial interest.

ACKNOWLEDGMENT

We thank the National Science Foundation (grant CHE - 1402004 to J.L.S.) and the Robert A. Welch Foundation for support. The work at Yonsei University was supported by Strategic Research (NRF-2016R1E1A1A01943379) through the National Research Foundation of Korea (NRF) funded by the Ministry of Science, ICT (Information and Communication Technologies) and Future Planning. We would like to thank Zhu-Lin Xie for help with the EPR measurements.

REFERENCES

(1) (a) Dougherty, D. A. *Acc. Chem. Res.* **1991**, *24*, 88. (b) Borden, W. T.; Iwamura, H.; Berson, J. A. *Acc. Chem. Res.* **1994**, *27*, 109. (c) Abe, M. *Chem. Rev.* **2013**, *113*, 7011. (d) Zeng, Z. B.; Shi, X. L.; Chi, C. Y.; Navarrete, J. T. L.; Casado, J.; Wu, J. S. *Chem. Soc. Rev.* **2015**, *44*, 6578.

(2) (a) Rawson, J. M.; Alberola, A.; Whalley, A. *J. Mater. Chem.* **2006**, *16*, 2560. (b) Iwasaki, A.; Hu, L. G.; Suizu, R.; Nomura, K.; Yoshikawa, H.; Awaga, K.; Noda, Y.; Kanai, K.; Ouchi, Y.; Seki, K.; Ito, H. *Angew. Chem., Int. Ed.* **2009**, *48*, 4022.

(3) Morita, Y.; Suzuki, S.; Sato, K.; Takui, T. *Nat. Chem.* **2011**, *3*, 197.

(4) (a) Kamada, K.; Ohta, K.; Kubo, T.; Shimizu, A.; Morita, Y.; Nakasuji, K.; Kishi, R.; Ohta, S.; Furukawa, S.; Takahashi, H.; Nakano, M. *Angew. Chem., Int. Ed.* **2007**, *46*, 3544. (b) Nakano, M.; Champagne, B. *J. Phys. Chem. Lett.* **2015**, *6*, 3236.

(5) Janoschka, T.; Hager, M. D.; Schubert, U. S. *Adv. Mater.* **2012**, *24*, 6397.

(6) (a) Dolphin, D.; Felton, R. H. *Acc. Chem. Res.* **1974**, *7*, 26. (b) Kadish, K. M.; Franzen, M. M.; Han, B. C.; Araullo-McAdams, C.; Sazou, D. *J. Am. Chem. Soc.* **1991**, *113*, 512. (c) Gross, Z.; Nimri, S. *J. Am. Chem. Soc.* **1995**, *117*, 8021. (d) G. Khoury, R.; Jaquinod, L.; M. Shachter, A.; Y. Nelson, N.; M. Smith, K. *Chem. Commun.* **1997**, 215. (e) Koide, T.; Kashiwazaki, G.; Suzuki, M.; Furukawa, K.; Yoon, M. C.; Cho, S.; Kim, D.; Osuka, A. *Angew. Chem., Int. Ed.* **2008**, *47*, 9661. (f) Ishida, M.; Shin, J.-Y.; Lim, J. M.; Lee, B. S.; Yoon, M.-C.; Koide, T.; Sessler, J. L.; Osuka, A.; Kim, D. *J. Am. Chem. Soc.* **2011**, *133*, 15533. (g) Gopalakrishna, T. Y.; Reddy, J. S.; Anand, V. G. *Angew. Chem., Int. Ed.* **2014**, 53, 10984. (h) Shimizu, D.; Oh, J.; Furukawa, K.; Kim, D.; Osuka, A. *Angew. Chem., Int. Ed.* **2015**, *54*, 6613. (i) Fukuzumi, S.; Ohkubo, K.; Ishida, M.; Preihs, C.; Chen, B.; Borden, W. T.; Kim, D.; Sessler, J. L. *J. Am. Chem. Soc.* **2015**, *137*, 9780. (j) Schweyen, P.; Brandhorst, K.; Wicht, R.; Wolfram, B.; Broring, M. *Angew. Chem., Int. Ed.* **2015**, *54*, 8213. (k) Shimizu, D.; Oh, J.; Furukawa, K.; Kim, D.; Osuka, A. *J. Am. Chem. Soc.* **2015**, *137*, 15584. (l) Yoshida, T.; Zhou, W.; Furuyama, T.; Leznoff, D. B.; Kobayashi, N. *J. Am. Chem. Soc.* **2015**, *137*, 9258.

(7) Caneschi, A.; Gatteschi, D.; Sessoli, R.; Rey, P. *Acc. Chem. Res.* **1989**, *22*, 392.

(8) Rath, H.; Tokuji, S.; Aratani, N.; Furukawa, K.; Lim, J. M.; Kim, D.; Shinokubo, H.; Osuka, A. *Angew. Chem., Int. Ed.* **2010**, *49*, 1489.

(9) Hisamune, Y.; Nishimura, K.; Isakari, K.; Ishida, M.; Mori, S.; Karasawa, S.; Kato, T.; Lee, S.; Kim, D.; Furuta, H. *Angew. Chem., Int. Ed.* **2015**, 54, 7323.

(10) Blusch, L. K.; Craigo, K. E.; Martin-Diaconescu, V.; McQuarters, A. B.; Bill, E.; Dechert, S.; DeBeer, S.; Lehnert, N.; Meyer, F. *J. Am. Chem. Soc.* **2013**, *135*, 13892.

(11) Hiroto, S.; Furukawa, K.; Shinokubo, H.; Osuka, A. *J. Am. Chem. Soc.* **2006**, *128*, 12380.

(12) Lash, T. D. *Chem. Rev.* **2017**, *117*, 2313.

(13) (a) Berlin, K.; Breitmaier, E. *Angew. Chem. Int. Ed. Engl.* **1994**, *33*, 1246. (b) Stępień, M.; Latos-Grażyński, L. *J. Am. Chem. Soc.* **2002**, *124*, 3838. (c) Stępień, M.; Latos-Grażyński, L. *Acc. Chem. Res.* **2005**, *38*, 88. (d) Lash, T. D. *Org. Biomol. Chem.* **2015**, *13*, 7846.

(14) Lash, T. D. *Angew. Chem. Int. Ed. Engl.* **1995**, *34*, 2533.

(15) (a) Lash, T. D.; Chaney, S. T. *Tetrahedron Lett.* **1996**, *37*, 8825. (b) Bergman, K. M.; Ferrence, G. M.; Lash, T. D. *J. Org. Chem.* **2004**, *69*, 7888.

(16) Lash, T. D.; Chaney, S. T. *Angew. Chem. Int. Ed. Engl.* **1997**, *36*, 839.

(17) (a) Lash, T. D.; Young, A. M.; Rasmussen, J. M.; Ferrence, G. M. *J. Org. Chem.* **2011**, *76*, 5636.(b) Szyszko, B.; Latos-Grażyński, L. *Organometallics* **2011**, *30*, 4354.

(18) (a) Furuta, H.; Asano, T.; Ogawa, T. *J. Am. Chem. Soc.* **1994**, *116*, 767. (b) Chmielewski, P. J.; Latosgrazynski, L.; Rachlewicz, K.; Glowiak, T. *Angew. Chem. Int. Ed. Engl.* **1994**, *33*, 779. (c) Toganoh, M.; Furuta, H. *Chem. Commun.* **2012**, *48*, 937.

(19) Lash, T. D.; Lammer, A. D.; Ferrence, G. M. *Angew. Chem., Int. Ed.* **2011**, 50, 9718.

(20) Gao, R.; AbuSalim, D. I.; Lash, T. D. *J. Org. Chem.* **2017**, *82*, 6680.

(21) (a) Sessler, J. L.; Seidel, D. *Angew. Chem., Int. Ed.* **2003**, *42*, 5134. (b) Saito, S.; Osuka, A. *Angew. Chem., Int. Ed.* **2011**, 50, 4342. (c) Sessler, J. L.; Gross, Z.; Furuta, H. *Chem. Rev.* **2017**, *117*, 2201. (d) Tanaka, T.; Osuka, A. *Chem. Rev.* **2017**, *117*, 2584. (e) Szyszko, B.; Białek, M. J.; Pacholska-Dudziak, E.; Latos-Grażyński, L. *Chem. Rev.* **2017**, *117*, 2839.

(22) (a) Mori, S.; Osuka, A. *J. Am. Chem. Soc.* **2005**, *127*, 8030. (b) Mori, S.; Kim, K. S.; Yoon, Z. S.; Noh, S. B.; Kim, D.; Osuka, A. *J. Am. Chem. Soc.* **2007**, *129*, 11344. (c) Kamimura, Y.; Shimizu, S.; Osuka, A. *Chem. Eur. J.* **2007**, *13*, 1620. (d) Tanaka, Y.; Saito, S.; Mori, S.; Aratani, N.; Shinokubo, H.; Shibata, N.; Higuchi, Y.; Yoon, Z. S.; Kim, K. S.; Noh, S. B.; Park, J. K.; Kim, D.; Osuka, A. *Angew. Chem., Int. Ed.* **2008**, *47*, 681. (e) Gokulnath, S.; Yamaguchi, K.; Toganoh, M.; Mori, S.; Uno, H.; Furuta, H. *Angew. Chem., Int. Ed.* **2011**, 50, 2302.

(23) AbuSalim, D. I.; Ferrence, G. M.; Lash, T. D. *J. Am. Chem. Soc.* **2014**, *136*, 6763.

(24) Anand, V. G.; Saito, S.; Shimizu, S.; Osuka, A. *Angew. Chem., Int. Ed.* **2005**, *44*, 7244.

(25) (a) Aviv-Harel, I.; Gross, Z. *Chem. Eur. J.* **2009**, *15*, 8382. (b) Teo, R. D.; Hwang, J. Y.; Termini, J.; Gross, Z.; Gray, H. B. *Chem. Rev.* **2017**, *117*, 2711. (c) Ghosh, A. *Chem. Rev.* **2017**, *117*, 3798. (d) Fang, Y.; Ou, Z.; Kadish, K. M. *Chem. Rev.* **2017**, *117*, 3377. (e) Orłowski, R.; Gryko, D.; Gryko, D. T. *Chem. Rev.* **2017**, *117*, 3102.

(26) (a) Simkhovich, L.; Mahammed, A.; Goldberg, I.; Gross, Z. *Chem. Eur. J.* **2001**, *7*, 1041. (b) Mahammed, A.; Gross, Z. *J. Inorg. Biochem.* **2002**, *88*, 305. (c) Palmer, J. H.; Day, M. W.; Wilson, A. D.; Henling, L. M.; Gross, Z.; Gray, H. B. *J. Am. Chem. Soc.* **2008**, *130*, 7786. (d) Buckley, H. L.; Anstey, M. R.; Gryko, D. T.; Arnold, J. *Chem. Commun.* **2013**, *49*, 3104.(e) Barata, J. F. B.; Neves, M. G. P. M. S.; Faustino, M. A. F.; Tomé, A. C.; Cavaleiro, J. A. S. *Chem. Rev.* **2017**, *117*, 3192.

(27) Wang, H.; Li, B.; Wu, H.; Hu, T.-L.; Yao, Z.; Zhou, W.; Xiang, S.; Chen, B. *J. Am. Chem. Soc.* **2015**, *137*, 9963.

(28) Adinarayana, B.; Thomas, A. P.; Suresh, C. H.; Srinivasan, A. *Angew. Chem., Int. Ed.* **2015**, 54, 10478.

(29) Szyszko, B.; Bialonska, A.; Szterenberg, L.; Latos-Grazynski, L. *Angew. Chem., Int. Ed.* **2015**, 54, 4932.

(30) (a) Klod, S.; Kleinpeter, E. *J. Chem. Soc., Perkin Trans. 2* **2001**, 1893. (b) Lu, T. *Multiwfn Software Manual, Vesrion 3.3.9,* Beijing Kein Research Center for Natural Sciences, Beijing,

China 2016. (c) Lu, T.; Chen, F. *J. Comput. Chem.* **2012**, *33*, 580.

(31) Krygowski, T. M.; Cyrański, M. K. *Chem. Rev.* **2001**, *101*, 1385.

(32) Krygowski, T. M.; Szatylowicz, H.; Stasyuk, O. A.; Dominikowska, J.; Palusiak, M. *Chem. Rev.* **2014**, *114*, 6383.

(33) Cho, S.; Lim, J. M.; Hiroto, S.; Kim, P.; Shinokubo, H.; Osuka, A.; Kim, D. *J. Am. Chem. Soc.* **2009**, *131*, 6412.

(34) (a) Furuta, H.; Maeda, H.; Osuka, A. *J. Am. Chem. Soc.* **2000**, *122*, 803. (b) Maeda, H.; Osuka, A.; Furuta, H. *J. Am. Chem. Soc.* **2003**, *125*, 15690.

(35) (a) Stępień, M.; Latos-Grażyński, L.; Lash, T. D.; Szterenberg, L. *Inorg. Chem.* **2001**, *40*, 6892. (b) Zhang, Z.; Ferrence, G. M.; Lash, T. D. *Org. Lett.* **2009**, *11*, 101. (c) Hong, J.-H.; Aslam, A. S.; Ishida, M.; Mori, S.; Furuta, H.; Cho, D.-G. *J. Am. Chem. Soc.* **2016**, *138*, 4992. (d) Białek, M. J.; Latos-Grażyński, L. *Inorg. Chem.* **2016**, 55, 1758.

(36) Khusnutdinova, J. R.; Rath, N. P.; Mirica, L. M. *J. Am. Chem. Soc.* **2010**, *132*, 7303.

(37) (a) Kim, D.; Osuka, A. *Acc. Chem. Res.* **2004**, *37*, 735. (b) Lee, S.; Mori, H.; Lee, T.; Lim, M.; Osuka, A.; Kim, D. *Phys. Chem. Chem. Phys.* **2016**, *18*, 3244.

(38) Fukui, N.; Cha, W.; Shimizu, D.; Oh, J.; Furukawa, K.; Yorimitsu, H.; Kim, D.; Osuka, A. *Chem.Sci.* **2017**, *8*, 189.

TOC graphic

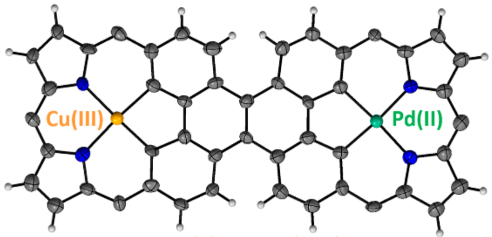

Stable π radical